Materials Science in Semiconductor Processing 102 (2019) 104604

Contents lists available at ScienceDirect

Materials Science in Semiconductor Processing

journal homepage: www.elsevier.com/locate/mssp

Effect of the Cu foam pretreatment in the growth and inhibition of copper oxide nanoneedles obtained by thermal oxidation and their evaluation as photocathodes

J. Edgar Carrera-Crespo[a,b], Ali M. Huerta-Flores[a], Leticia M. Torres-Martínez[a,*], Isaías Juárez-Ramírez[a]

[a] Universidad Autónoma de Nuevo León, UANL, Facultad de Ingeniería Civil, Departamento de Ecomateriales y Energía, Av. Universidad S/N Ciudad Universitaria, San Nicolás de los Garza, Nuevo León, C.P. 66455, Mexico

[b] Unidad Profesional Interdisciplinaria de Biotecnología, Instituto Politécnico Nacional, Av. Acueducto 550, La Laguna Ticomán, 07340, Ciudad de México, Mexico

ARTICLE INFO

Keywords:
Copper oxide nanoneedles
Thermal oxidation
Growth mechanism
Substrate pretreatment

ABSTRACT

Cu_2O-CuO layers were prepared in situ on copper foam substrates by thermal oxidation at 400 °C in air using different pretreatments with acetone, HCl and NaOH. The effect of the pretreatment in the shape and physicochemical properties of the Cu_2O-CuO layers, as well as in the growth or inhibition of the copper oxide nanostructures was studied, and a growth mechanism is proposed. It was found that the pretreatment modulates the nucleation and growth of the copper oxide nanostructures, being the process with NaOH the most suitable to promote the formation of well-defined nanoneedles, while in the case of the samples pretreated with acetone and HCl, copper oxide layers with irregular shape microstructures were obtained. The composition, structural, morphological and optical properties of the copper oxide structures were determined by X-ray diffraction, scanning electron microscopy, UV-vis diffuse reflectance and photoluminescence spectroscopy. The results showed that in all cases, the presence of both copper oxides, Cu_2O and CuO was observed, with an optical band gap of 1.0 and 1.3 eV. The copper oxide structures exhibited photoluminescence emission centered at 551 nm, related to the recombination of the electron-hole pairs in the samples. The materials prepared with a NaOH pretreatment showed the lower emission and recombination rate.

Moreover, the 3D Cu-Cu_2O-CuO based materials were evaluated as photocathodes in a 0.5 M Na_2SO_4 solution and under Xe lamp illumination. The photoelectrode where 1D nanostructures were grown, exhibited the lower resistance to the charge transference in the Nyquist plots, the highest current density in the linear voltammetry and the highest photoresponse in the on-off light experiments. The improved electrical and physicochemical properties of the samples pretreated with NaOH was related to the particular 1D nanoneedle morphology, which promoted higher conductivity and photoresponse, lower resistance to the charge transference and lower recombination of free charge carriers, demonstrating the potential use of these electrodes for photoelectrochemical applications. Finally, this work proved that it is possible to grow well-defined and highly crystalline CuO nanoneedles on copper foam porous substrates through a simple, fast and clean method.

1. Introduction

1D nanostructured copper oxides have attracted attention recently due to their potential use in several applications such as cathodes for lithium-ion batteries [1,2], gas sensors [3] and biosensors [4,5], catalysts [6] and photocatalysts [7], as well as photocathodes for hydrogen generation from water [8,9], since cuprous and cupric oxides are usually p-type semiconductors, with a direct band gap of approximately 2.0–2.5 eV and 1.3–1.7 eV, respectively [10]. Moreover, these nanostructures are obtained from copper, an earth-abundant metal, and can be synthesized through facile and scalable methods such as simple thermal oxidation of the copper substrate [3,7,11]. Typically, copper oxide structures in the form of nanowires or nanoneedles are grown on copper substrates by thermal annealing at temperatures between 400 °C and 600 °C in air or oxygen atmospheres [12]. CuO wires, sheets and flower nanostructures have been grown on copper foam substrates and studied as supercapacitors [13], while in other work, highly porous CuO structures for batteries and fuel cells were sculptured tunning the

* Corresponding author.
E-mail address: leticia.torresgr@uanl.edu.mx (L.M. Torres-Martínez).

https://doi.org/10.1016/j.mssp.2019.104604
Received 25 February 2019; Received in revised form 29 June 2019; Accepted 2 July 2019

pore sizes through the variation of the deposition conditions [14]. The scalable and facile anodization-calcination process was used also for the preparation of copper oxide anodes for ion-lithium batteries [15]. Moreover, the copper-based nanostructures prepared by this method have exhibited high selectivity, sensitivity and stability for gas sensing applications [16]. The shape of the nanostructures has been also modified through the use of surfactants, such as Triton X-100, for obtaining cabbage rose CuO structures on copper foam substrates [17], and core-shell CuO-NiO hybrid structures with enhanced supercapacitance performance have been prepared [18]. Organic-inorganic nanocomposites based on CuO have showed high electrical conductivity, good mechanical strength and excellent properties as catalysts for the oxidation of CO and NO [19–22], highlighting the multifunctional properties and versatile applications of CuO nanostructures.

On the other hand, it has been reported that the growth and characteristics of these nanostructures are influenced by parameters such as the annealing time [3,13], temperature [11,23–26], atmosphere [27–29], the grain size and orientation of the copper substrate [30–32]. Another critical factor in the features of an oxide thermally grown is the surface morphology of the substrate, which can be modified during the metal substrate pretreatment, but the effect of this parameter has not been considered in the synthesis of 1D copper oxide nanostructures. Generally, copper substrates are pretreated in HCl solutions to remove the native oxide and other impurities, or polished with fine sandpaper, subsequently rinsed with water and acetone and finally dried in N_2 or air before their thermal oxidation [22]. If is compared the pretreatment used by Zhong et al. [23], which consisted in the polished of the copper foil substrate, with the used by Li et al. [1], where the copper foil was pretreated in HCl, the first one should have a higher surface rugosity than the last one. Then, since the composition and thickness of the copper foils were similar, the differences observed in the shape, amount and distribution of the nanowires could be associated to the applied pretreatment, but the variations in the annealing time and temperature could also have an effect on these features, hindering the comparison.

For this reason, in this work is evaluated the pretreatment effect in the growth, shape, distribution, and properties of the copper oxide layer and nanostructures obtained by thermal oxidation of a copper foam, at 400 °C for 2 h in an atmosphere of air. Cu foam, a 3D metallic skeleton, was selected as a substrate due to its high porosity and higher surface area than the Cu foil [2], making it a suitable matrix to support copper oxides and other semiconductors to obtain photocathodes more efficient for photoelectrochemical applications. Therefore, the photoelectrodes obtained by the different pretreatments and subsequently thermal oxidation were (photo)electrochemically evaluated. Also, based on the results obtained, a growth mechanism of the nanoneedles is proposed, evidencing that the pretreatment is a crucial factor that can promote or inhibit the formation of 1D copper oxide nanostructures.

2. Experimental methods

2.1. Fabrication of the copper oxide structures

For the preparation of the copper oxide nanostructures, copper foam pieces (5 mm × 20 mm) from Nanoshel (Purity: 99%, Porosity: 80%, Thickness: 4 mm, Density: 850 g/m^2) were used as substrates. The pieces were cleaned in an ultrasonic bath for 10 min using 20 mL of acetone (95%, Reactivos y Equipos). Then, the pieces were treated chemically employing an acid and basic solution, in order to evaluate the effect of this pretreatment in the composition and structural features of the copper oxide layer obtained after the thermal treatment of the metallic foam. A piece of copper foam was immersed in an aqueous solution of 10 wt% HCl, keeping the sample in an ultrasonic bath for 10 min. Another piece was treated in a solution of 1 M NaOH, using the same time of ultrasonication. After the treatment, the samples were rinsed thoroughly with deionized water. Then, the samples were placed in an alumina crucible, and they were thermally oxidized in air at 400 °C for 2 h. A sample of copper foam cleaned in acetone and annealed in air at the same conditions than the other samples was used as a reference. For the facility, the samples are referred in the manuscript as TO-Cu:Ac, TO-Cu:Ac/HCl, and TO-Cu:Ac/NaOH to describe the reference sample and the samples treated chemically, respectively.

2.2. Characterization of the structures

The structural features of copper oxide, obtained after the thermal treatment of the metallic foams, were studied through X-ray diffraction in a Bruker D8 diffractometer (CuKα radiation λ = 1.5418 Å), collecting the data from 30° to 70°, using a scan rate of 0.05°. The XRD analysis were performed on grazing incidence angle mode, using a fixed incident angle of 1°. The microstructure of the samples was explored with a scanning electron microscope from JEOL Instruments (JSM 6490). The optical properties were analysed using a UV-Vis NIR spectrophotometer (Cary 5000) coupled with an integration sphere and a photoluminescence spectrophotometer (Agilent Cary Eclipse), employing a scan speed of 1000 nm/min and an excitation wavelength of 350 nm. The electrochemical characterization was performed in a Metrohm AUTOLAB (model PGSTAT302 N) potentiostat-galvanostat system, equipped with a Frequency Response Analyzer (FRA) module, using a three-electrode cell equipped with a quartz window. A solution of 0.5 M Na_2SO_4 was used as electrolyte, a platinum wire and an Ag/AgCl electrode were employed as counter and reference electrode, respectively. The 3D metallic foams containing the copper oxide structures, with an exposed geometrical area in solution of 0.65 cm^2, were used as working electrodes. The illumination was provided by a 100 W Xe lamp, enclosed in a Newport Q Housing model 60025. Electrochemical impedance spectroscopy (EIS) characterization was carried out under illumination, at −0.3 V vs. Ag/AgCl, with AC perturbation of ± 10 mV, in a frequency range of 100 kHz to 1 Hz.

3. Results and discussion

3.1. Morphological characterization

Fig. 1 shows the SEM images of the copper foams after the pretreatment in the different solutions. The copper foam surface before pretreatments is similar to the exhibited for the sample pretreated only in acetone (Fig. 1a–c), where slight asperities associated with the native layer of copper oxide were detected. These asperities are not observed on the surface of the Cu foam pretreated in 10 wt%. HCl, being evident the formation of small holes with a shape of rectangles and circles, as well as deeper copper grain boundaries, due to the erosion and etching caused by the acid solution on this surface (Fig. 1d–f). On the other hand, a thin layer of copper oxide with high roughness is formed on the surface of the Cu foam pretreated in 1 M NaOH (Fig. 1g–i). To elucidate only the effect of the pretreatments in the features of the copper oxide grown by thermal oxidation, the pretreated Cu foam samples were annealed at 400 °C in air for 2 h. Fig. 2 shows the SEM images of the samples after the thermal treatment, where it can be appreciated differences in the copper oxide layer morphology formed on the walls of the Cu foams. Although at higher magnifications the copper oxide layer is grown on the Cu foams pretreated in acetone (TO-Cu:Ac), and 10 wt% HCl (TO-Cu:Ac/HCl) seem to be similar (Fig. 2a–d and e-h, respectively), in the first one few nanoneedles were observed on the surface of the copper oxide layer whereas in the last one were not detected. This result is notable, since these nanostructures have been synthesized on copper substrates pretreated in HCl solutions and annealed in air at the same temperature but for 4 h [11,26]. Possibly, the way in that the pretreatment in HCl solutions is given also affects the surface morphology of the copper substrate, since C. Wang et al. [11] and Y. Wang et al. [26] used 1 M HCl and dilute HCl, respectively, to clean the copper substrate, and in this work, the copper foam was cleaned in 10 wt% HCl under sonication for 10 min.

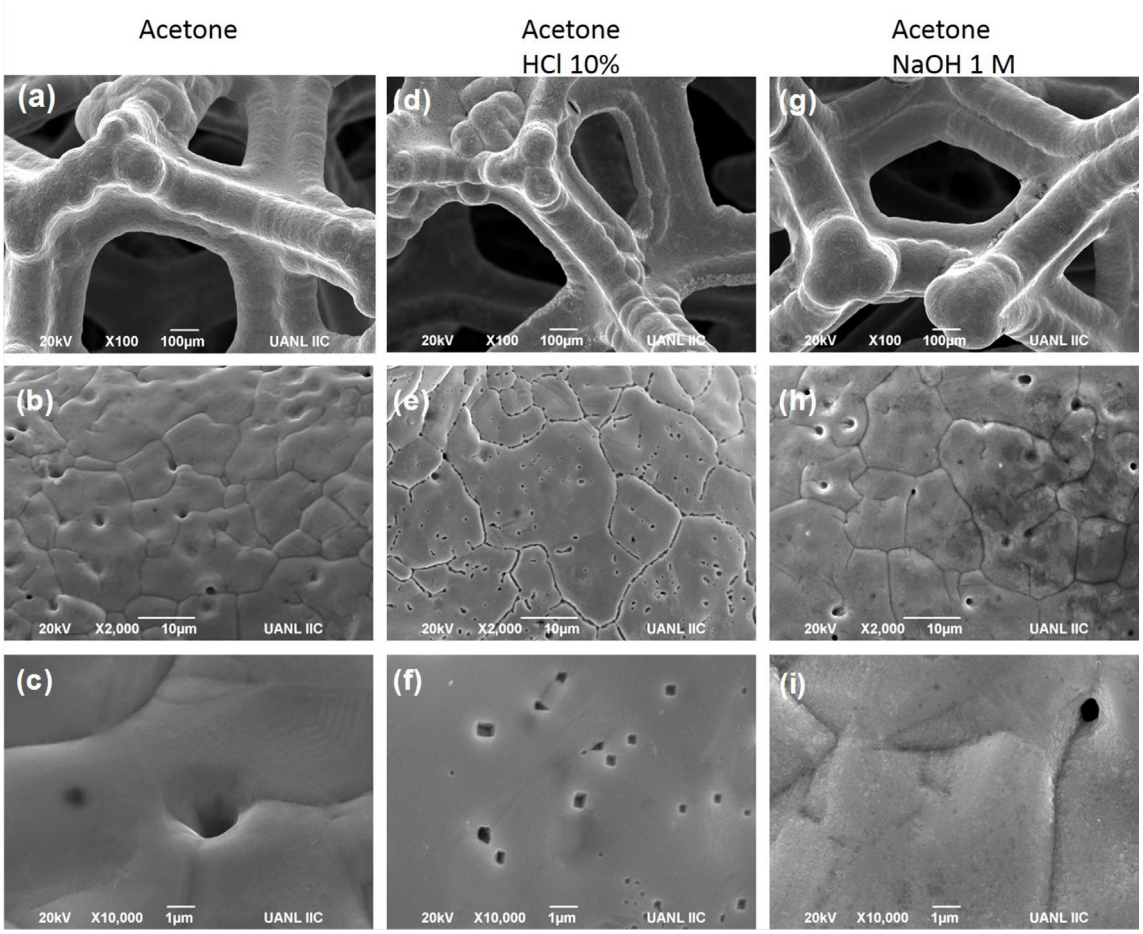

Fig. 1. SEM images of the copper foam substrates after the pretreatment with (a–c) acetone, (d–f) 10 wt% HCl, and (g–i) 1 M NaOH.

As a result, the copper oxide layer grown on the Cu foam pretreated in 1 M NaOH (TO-Cu:Ac/NaOH) shows a distinct morphology with a large number of nanoneedles on its surface (Fig. 2i-l). These variations indicate that the pretreatment has a great influence in the morphology of the copper oxide layer, as well as in the inhibition or growth of copper oxide nanostructures, since the pretreatment in 10 wt% HCl let a copper oxide surface free of nanoneedles and the pretreatment in 1 M NaOH promoted the growth of these nanostructures. The compositional homogeneity of the structures was corroborated through EDS analysis (Fig. S1), where only Cu and O elements were detected. Moreover, the elemental mappings included in Fig. S2 demonstrate the homogeneous distribution of copper and oxygen on the substrates.

3.2. Structural and compositional analysis

To elucidate the composition of the copper oxide grown on the walls of the Cu foams pretreated in the different solutions, the samples were analysed by XRD (Fig. 3). In the XRD pattern of Cu foam without pretreatments (Fig. 3a), only two peaks associated with metallic copper are detected at $2\theta = 43.5^{\circ}$ and 50.6° [11]. Along with these peaks, other new peaks were identified in the diffractograms after annealing of samples. These peaks at $2\theta = 35.5^{\circ}$, 38.8°, 48.7°, 66.1°, 67.9°, and $2\theta = 36.4^{\circ}$, 42.2°, 61.2°, are associated to the CuO [11] and Cu_2O [31], respectively. The TO-Cu:Ac and TO-Cu:Ac/HCl (Fig. 3b and c) samples show similar diffractograms, where the peaks of the Cu_2O exhibit a higher intensity than the peaks of the CuO, being the peaks of this last one located at $2\theta = 35.5^{\circ}$, 48.7°, 66.1° and 67.9° almost undetectable in both XRD patterns. These peaks are more noticeable in the diffractogram obtained by the TO-Cu:Ac/NaOH sample (Fig. 3d), suggesting that the nanoneedles grown on its copper oxide layer are composed of CuO phase, as has been reported in some works where these nanostructures were obtained through thermal oxidation of copper substrates [1,7,23,25]. Then, the copper oxide layer could be mainly formed of Cu_2O, since the peaks related to this oxide are more intense than the CuO in the samples where the presence of nanoneedles was minimal or null. Moreover, the presence of Cu_2O in the bottom of the oxide layer is more possible if it is taking into account the oxidation of metal copper in the air [1].

According to the results obtained in the characterization by SEM and XRD, we propose a growth mechanism of the nanoneedles which is shown in Fig. 4. The different pretreatments caused modifications on the surface of the Cu foam substrates; therefore, due to the thermal oxidation was carried out at the same conditions, the changes observed only can be attributed to this process. The native copper oxide layer with slight asperities remains after the pretreatment in acetone (Fig. 1a–c), whereas it is removed in the Cu foam pretreated in 10 wt% HCl, leaving a surface without visible asperities (Fig. 1d–f). On the other hand, several asperities are detected on the rough, thin copper oxide layer formed after the pretreatment in 1 M NaOH (Fig. 1g–i). Then, these asperities seem to be linked to the growth and quantity of CuO-nanoneedles on the copper oxide layer, since a minimum (Fig. 2a–d) and a large amount (Fig. 2i-l) of these nanostructures were detected in the samples with slight and several asperities, respectively; whereas their growth was inhibited in the sample where the asperities were removed (Fig. 2e–h). This behaviour suggests that the asperities provoke defects on the surface of the thermally formed copper oxide layer that act as seeding sites to the nanoneedles, since on the surface of the TO-Cu:Ac/NaOH sample can be observed small nuclei around to 50

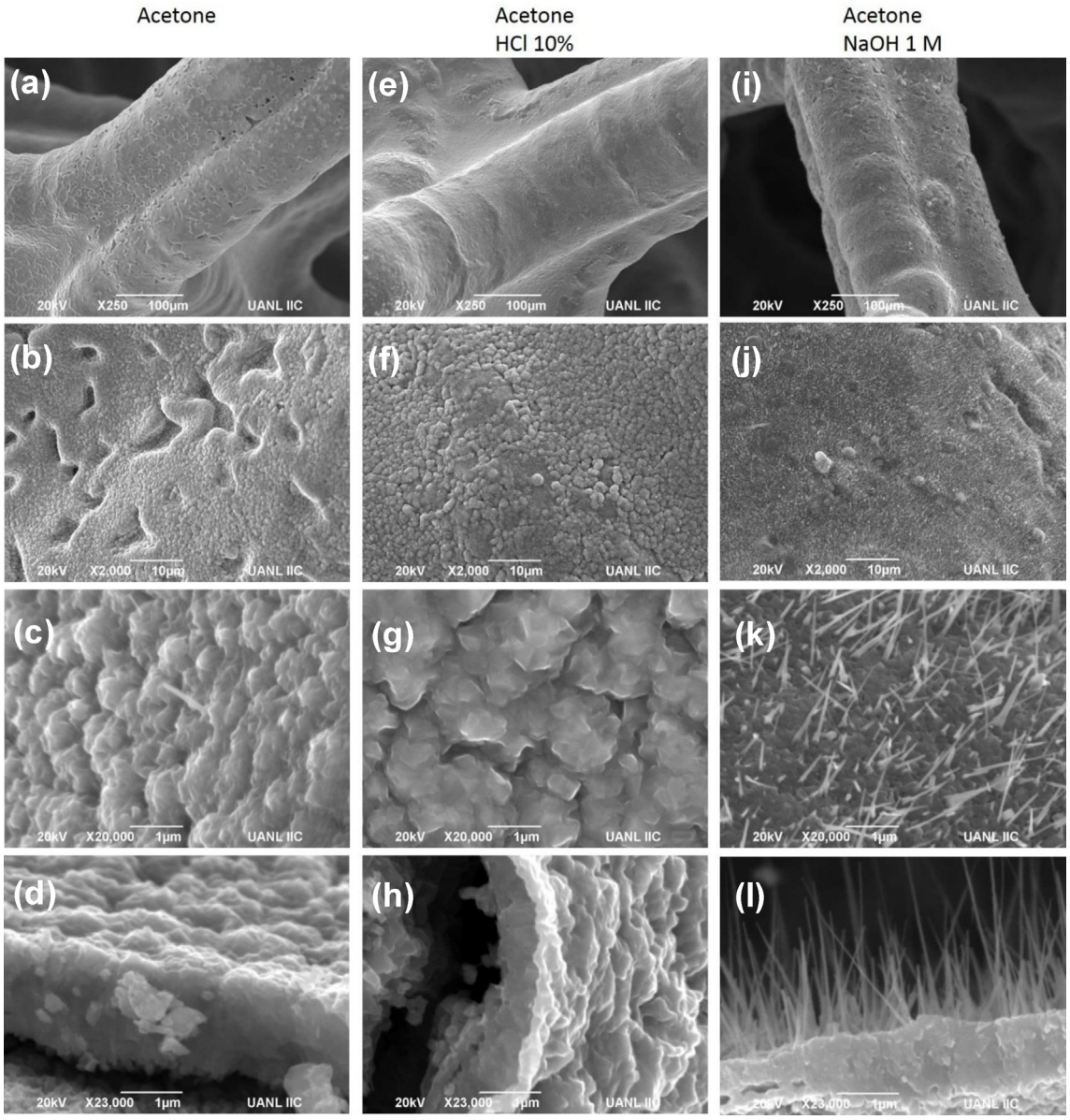

Fig. 2. SEM images of the samples pretreated with (a–d) acetone, (e–h) 10 wt% HCl, and (i–l) 1 M NaOH after the annealing at 400 °C for 2 h.

and 100 nm where new nanoneedles are growing (Fig. 2k). Moreover, the rough surface of the copper oxide layer in this sample is similar to the surface of the thin copper oxide layer formed through the pretreatment in 1 M NaOH (Fig. 1i), indicating that the morphology of the thermally formed copper oxide layer was influenced for the presence of the first layer of oxide.

Lattice and grain-boundary diffusion mechanisms have been proposed to explain the thermal growth of copper oxide on Cu substrates, where the first let a continuous increase of the Cu_2O and CuO layers, and the second let the formation and growth of nanostructures such as nanowires or nanoneedles [12,23]. Additionally, to the grain-boundary diffusion, the results obtained in this work indicate that is necessary the presence of seeding sites, which can be promoted or inhibited through the pretreatment given to the Cu substrate, to reach the formation of these nanostructures on the copper oxide layer.

3.3. Optical properties of the copper oxide structures

To elucidate the optical properties and (photo)electrochemical behaviour of the copper oxide layers with and without nanoneedles on their surface, the TO-Cu:Ac, TO-Cu:Ac/HCl and TO-Cu:Ac/NaOH samples were characterized by DRS and evaluated as (photo)electrodes.

The UV-Vis spectra of copper oxide nanostructures prepared under different conditions are shown in Fig. 5a. The samples exhibit an optical spectrum with absorption in the ultraviolet, visible and near-infrared range, and a well-defined absorption edge near to 950 nm–1000 nm. From this figure, the optical band gap of the samples was calculated. Band gap values of 1.0 eV, 1.1 eV, and 1.3 eV were obtained for TO-Cu:Ac, TO-Cu:Ac/HCl, and TO-Cu:Ac/NaOH, respectively. The obtained spectra and band gap values are similar to those reported for CuO [33–36]. XRD patterns evidenced the presence of both CuO and Cu_2O phases. Cu_2O exhibit a larger band gap (~2 eV) [37–40], which is not similar to the observed in the samples. In the oxidation process, first, Cu substrate is oxidized to Cu_2O, and then Cu_2O is oxidized to CuO. It is probably that the annealing process promoted the oxidation of the surface layers, leaving an intern layer of Cu_2O. The XRD analysis penetrates both surface and internal layer and demonstrates the presence of both phases. But in the UV-Vis diffuse reflectance measurement, the external layer of CuO is the most representative in the analysis, leading to an absorption spectra similar to CuO. Accordingly, the sample that

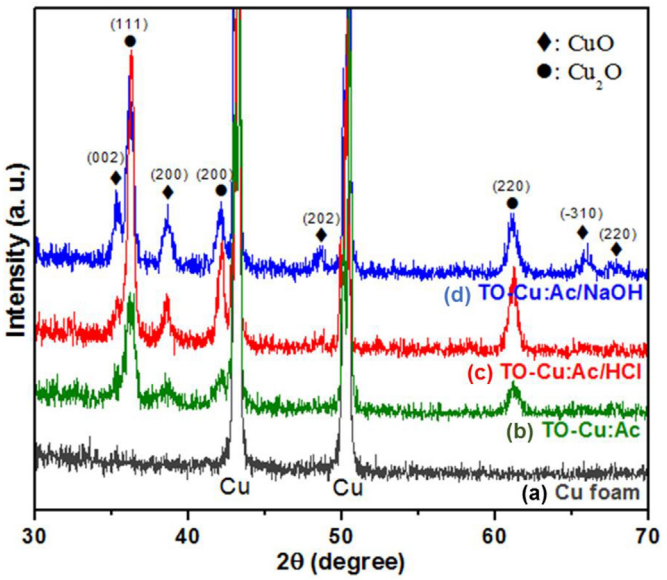

Fig. 3. XRD patterns of (a) Cu foam, and the samples pretreated with (b) acetone, (c) 10 wt% HCl and (d) 1 M NaOH, identified as TO-Cu:Ac, TO-Cu:Ac/HCl, and TO-Cu:Ac/NaOH, respectively.

exhibited major formation of CuO, TO-Cu:Ac/NaOH, showed higher absorbance in the optical spectra.

Fig. 5b presents the photoluminescence spectra of the samples excited at 350 nm. The samples exhibit a photoluminescence peak centered at 550 nm, corresponding to the green spectral range. This is indicative of a possible application for visible light-emitting devices. An important observation is that the UV-Vis spectra show representative spectra of CuO, while, the band to band transition observed in PL spectra (~2 eV) is characteristic of Cu_2O. This could be due to the excitation energy that we used in the measurement (350 nm), which is enough to promote the excitation of Cu_2O with a larger band gap.

The peak observed is attributed to the recombination of the electron-hole pairs in the nanostructures, where a higher intensity of the peak involves higher recombination [41–45]. The PL intensity observed in the samples shows the following tendency: TO-Cu:Ac/NaOH < TO-Cu:Ac/HCl < TO-Cu:Ac, which implies that the pretreatment with NaOH promotes the formation of copper oxide nanoneedles with improved properties for the charge separation and transport, reducing electron-hole pair recombination, a favorable feature for optical and photo(electro)catalytic applications.

3.4. Photoelectrochemical characterization

Fig. 6a shows the OCP variation over time of the studied electrodes in the dark and under illumination. The OCP values, obtained in dark conditions, tend towards more negative potentials when the amount of nanoneedles is increased on the electrodes surface, since the OCP of the TO-Cu:Ac is slightly more negative than TO-Cu:Ac/HCl, being the most negative OCP the obtained by TO-Cu:Ac/NaOH electrode, this could be attributed to the higher concentration of n-type Cu_2O [46]. Although the OCP values reached under illumination are similar for the three electrodes, the difference between the OCP obtained in the dark and under illumination is greater for the TO-Cu:Ac/NaOH, indicating a higher generation of charge carriers in this electrode. Linear sweep voltammetry was carried out from OCP to −0.3 V *vs.* Ag/AgCl, under dark and illumination conditions. The current densities obtained in the dark are much smaller than those generated under lighting for the three electrodes (Fig. 6b), evidencing a good photoactivity of these materials, specially of the TO-Cu:Ac/NaOH electrode, where the nanoneedles were grown in greater quantity, which reached a photocurrent near to −5 mA/cm^2 at −0.3 V *vs.* Ag/AgCl. However, when this potential is fixed and the photocathodes illuminated, the photocurrent decay to values close to −2 mA/cm^2 for the three electrodes (Fig. 6c), probably due to recombination processes that could be associated with the copper oxide film grown on the surface of metallic copper (Fig. 2 d, h and l), since in all the electrodes the current suddenly decreases immediately after they are illuminated. Despite this, the photocurrent reached by TO-Cu:Ac/NaOH photocathode was the most stable and the higher after 10 cycles of dark:light by 1 min:1 min (Fig. 6c).

In order to elucidate the effect of the nanoneedles in the electrical properties of the photocathodes, these were characterized by electrochemical impedance spectroscopy (EIS) at −0.3 V *vs.* Ag/AgCl and under lighting conditions. The Nyquist diagrams obtained by each

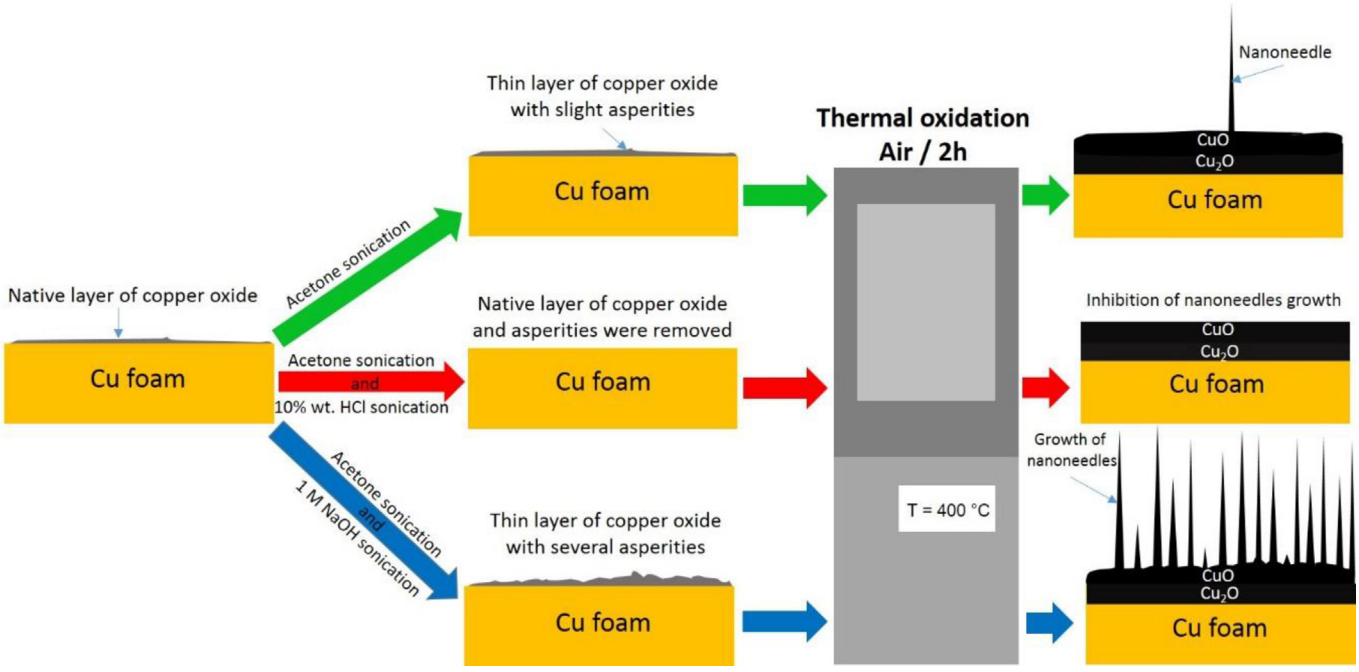

Fig. 4. Mechanism of growth of the copper oxide nanostructures on Cu foam substrate pretreated in different conditions.

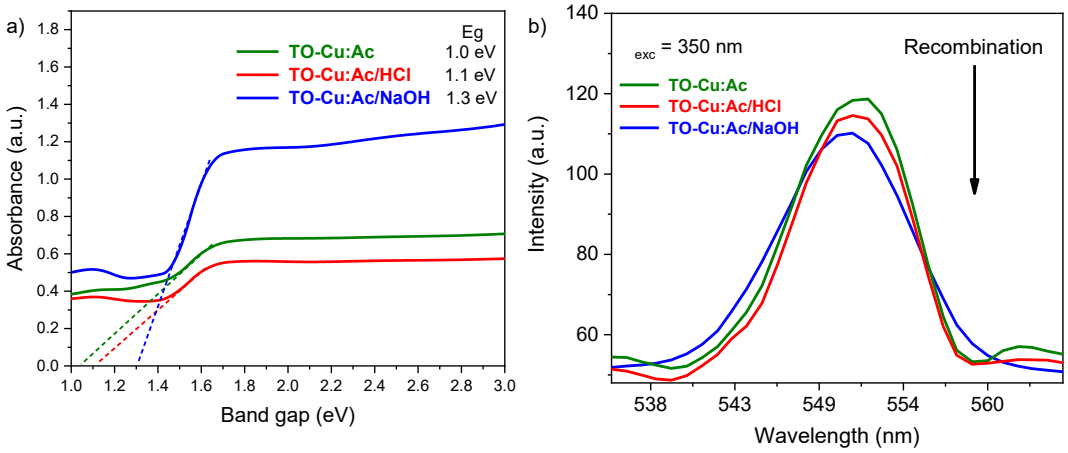

Fig. 5. (a) UV-Vis spectra and (b) Photoluminescence curves of TO-Cu:Ac, TO-Cu:Ac/HCl, and TO-Cu:Ac/NaOH electrodes.

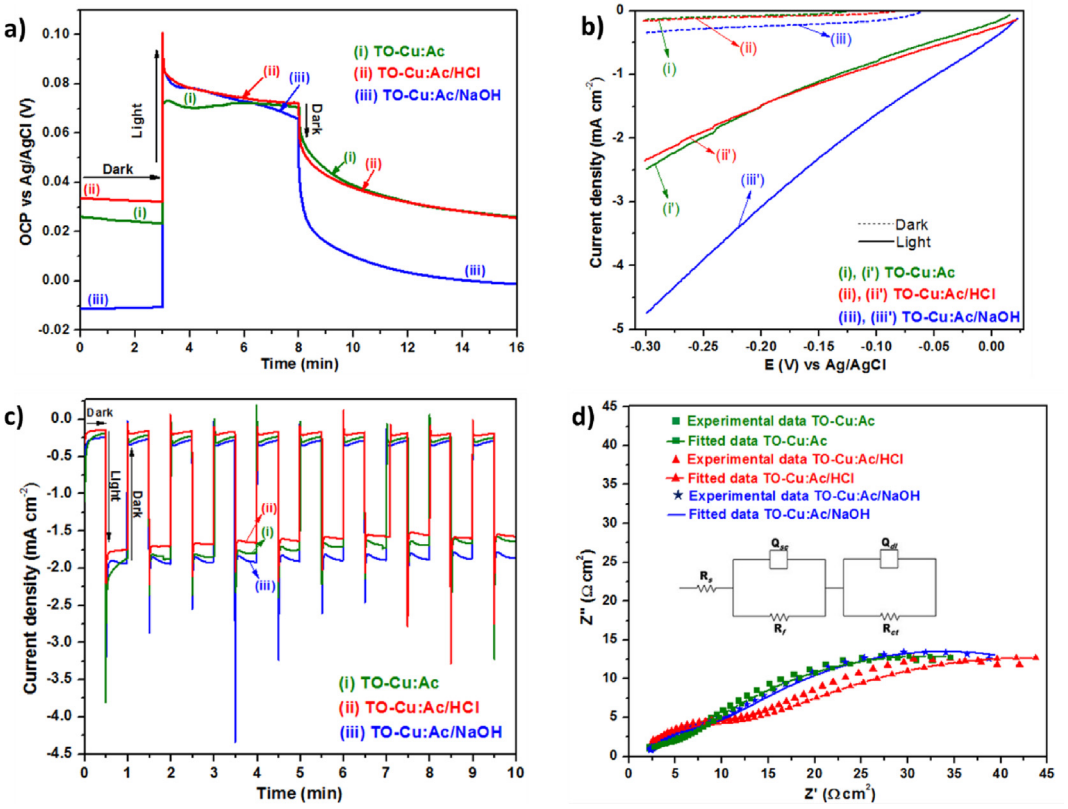

Fig. 6. (a) OCP variation over time, (b) Current density in the dark and in the light, (c) On-off current density measurements obtained at −0.3 V vs. Ag/AgCl, and (d) Nyquist plots of the copper oxide structures prepared by thermal oxidation.

Table 1
Parameters obtained from the fitting of experimental EIS data obtained at −0.3 V *vs.* Ag/AgCl under illumination conditions, using the equivalent electric circuit shown in Fig. 6d.

Electrode	R_s (Ω cm^2)	R_f (Ω cm^2)	Q_{sc} (mho s^n cm^{-2}) (10^{-4})	n	R_{tc} (Ω cm^2)	Q_{dl} (mho s^n cm^{-2}) (10^{-3})	n
TO-Cu:Ac	1.3	3.9	7.69	0.62	53.7	5.6	0.57
TO-Cu:Ac/HCl	0.67	10.2	3.3	0.61	64.5	6.2	0.47
TO-Cu:Ac/NaOH	1.73	7.1	7.8	0.66	51.1	4.6	0.61

photocathode and the electrical equivalent electric circuit (*eec*) used to fit the experimental data are shown in Fig. 6d, where Rs, Rf, and Rct, are the electrolyte resistance, charge transport resistance, and charge transfer resistance, respectively. Qsc and Qdl are constant phase elements (CPE) associated with the space charge capacitance and double layer capacitance, respectively [47–49]. The parameters obtained by fitting experimental data employing the Zview software are shown in Table 1. The highest values of Rf and Rct were obtained for the electrode where the growth of nanoneedles was inhibited, indicating that the presence of these nanostructures improved the electrical properties of the Cu-Cu_2O-CuO based photocathodes, and thus, increased their photoelectrochemical performance, as confirmed by the photocurrent results obtained at −0.3 V *vs.* Ag/AgCl (Fig. 6c). The n-type conductivity of Cu_2O and p-type conductivity of CuO was corroborated

through Mott Schottky plots, included in Fig. S1 in Supporting Information. The presence of CuO promotes the formation of a p-n heterostructure between p-type CuO and n-type Cu_2O, reducing the recombination of charges and allowing a faster transference in the interface, which enhanced electron conductivity and lower resistance in the electrode. In the formed heterostructure, the electrons in Cu_2O are transferred to the conduction band of CuO, and the holes move in the inverse direction [50].

The role of the copper foam is to act as a conductive support and as precursor for the formation of copper oxide nanostructures. Considering that these materials are being evaluated as photocathodes, the light absorption capacity is very important. For this reason, the 3D structure of the foam support provides an interconnected three-dimensional structure with enhanced charge transport properties and where the light trapping phenomena can take place, promoting a major light absorption and conversion. The process to obtain the copper oxide nanostructures used in this work can be applied on Cu bulk, but for their use as photocathodes they must be deposited in a conductive support.

4. Conclusions

In summary, in this work 1D CuO nanoneedles were successfully grown on copper porous and high-surface-area foam substrates by a fast and easy thermal oxidation method. The physicochemical analysis showed that the mixed phases Cu_2O-CuO in all the structures were obtained. The use of different pretreatments modified the processes of nucleation and growth of the materials, favoring the formation of different morphologies. The pretreatment with NaOH was found to be the most suitable to promote the growth of 1D nanoneedles, while in the case of the foams pretreated with acetone and HCl, only irregular shaped structures were observed. During the use of the Cu-Cu_2O-CuO based electrodes as photocathodes, the oxides with nanoneedle morphology exhibited the highest photoresponse and current density, as well as the lower resistance to the charge transference. The improved properties of CuO nanoneedles were adjudicated to the unique 1D morphology obtained in the samples pretreated with NaOH, which allows the enhancement of the electrical and physicochemical properties. In summary, this work demonstrated that the pretreatment is a crucial factor to promote or inhibit the growth of copper oxide nanoneedles through a simple method such as thermal oxidation, improving these nanostructures the photoelectrochemical performance of the Cu-Cu_2O-CuO based electrodes, making them promising materials for multiple optical, electronic and photo(electro)catalytic applications.

Acknowledgments

J.E. Carrera-Crespo thank CONACYT for the economic support to pursue his postdoctoral studies. The authors would like to thank CONACYT (CB-2014-237049, CB-2015-256645, CB-2016-256795) PDCPN-2015-01-105, PDCPN-2015-01-487, NRF-2016-278729, and PhD Scholarship 386267), SEP-PROFIDES 511-6/18-11852, UANL (PAICYT 2018 IT633-18, PAICYT 2019 IT325-19), and FIC-UANL (PAIFIC 2018-5 and PAIFIC-UANL-2018-12).

Appendix A. Supplementary data

Supplementary data to this article can be found online at https://doi.org/10.1016/j.mssp.2019.104604.

References

[1] A. Li, et al., Copper oxide nanowire arrays synthesized by in-situ thermal oxidation as an anode material for lithium-ion batteries, Electrochim. Acta 132 (2014) 42–48.
[2] J. Li, et al., Thermally oxidation synthesis of CuO nanoneedles on Cu foam and its enhanced lithium storage performance, J. Mater. Sci. Mater. Electron. 28 (3) (2016) 2353–2357.
[3] F. Shao, et al., Copper (II) oxide nanowires for p-type conductometric NH3 sensing, Appl. Surf. Sci. 311 (2014) 177–181.
[4] W. Lu, et al., Direct growth of pod-like Cu 2 O nanowire arrays on copper foam: highly sensitive and efficient nonenzymatic glucose and H 2 O 2 biosensor, Sensor. Actuator. B Chem. 231 (2016) 860–866.
[5] S. Yang, et al., Synthesis of nanoneedle-like copper oxide on N-doped reduced graphene oxide: a three-dimensional hybrid for nonenzymatic glucose sensor, Sensor. Actuator. B Chem. 238 (2017) 588–595.
[6] R.L. Papurello, et al., Microreactor with copper oxide nanostructured films for catalytic gas phase oxidations, Surf. Coating. Technol. 328 (2017) 231–239.
[7] V. Scuderi, et al., Photocatalytic activity of CuO and Cu2O nanowires, Mater. Sci. Semicond. Process. 42 (2016) 89–93.
[8] P. Wang, Y.H. Ng, R. Amal, Embedment of anodized p-type Cu(2)O thin films with CuO nanowires for improvement in photoelectrochemical stability, Nanoscale 5 (7) (2013) 2952–2958.
[9] J. Luo, et al., Cu2O nanowire photocathodes for efficient and durable solar water splitting, Nano Lett. 16 (3) (2016) 1848–1857.
[10] Y. Yang, et al., Cu2O/CuO bilayered composite as a high-efficiency photocathode for photoelectrochemical hydrogen evolution reaction, Sci. Rep. 6 (2016) 35158.
[11] C. Wang, et al., Cupric oxide nanowires on three-dimensional copper foam for application in click reaction, RSC Adv. 7 (2017) 9567–9572.
[12] G. Filipic, U. Cvelbar, Copper oxide nanowires: a review of growth, Nanotechnology 23 (19) (2012) 194001.
[13] Y. Li, et al., Nanostructured CuO directly grown on copper foam and their supercapacitance performance, Electrochim. Acta 85 (2012) 393–398.
[14] H.C. Shin, et al., Copper foam structures with highly porous nanostructured walls, Chem. Mater. 16 (2004) 5460–5464.
[15] Z. Wang, et al., Yucca tern shaped CuO nanowires on Cu foam for remitting capacity fading of Li-ion battery anodes, Sci. Rep. 8 (2018) 6530.
[16] A. Rydosz, et al., The use of copper oxide thin films in gas-sensing applications, Coatings 8 (2018) 425.
[17] P.E. Lokhande, et al., Surfactant-assisted cabbage rose-like CuO deposition on Cu foam by for supercapacitor applications, Inorganic and Nano-Metal Chemistry 8 (9) (2018) 434–440.
[18] M. Huang, et al., Hierarchical NiO nanoflake coated CuO flower core-shell nanostructures for supercapacitor, Ceram. Int. 40 (2014) 5533–5538.
[19] Q. Zhang, et al., CuO nanostructures: synthesis, characterization, growth mechanisms, fundamental properties, and applications, Prog. Mater. Sci. 60 (2014) 208–337.
[20] M. Vaseem, et al., Low-Temperature Synthesis of flower-shaped CuO nanostructures by solution process: formation mechanism and structural properties, J. Phys. Chem. C 112 (2008) 5729–5735.
[21] L. Xu, et al., Novel urchin-like CuO synthesized by a facil reflux method with efficient olefin epoxidation catalytic performance, Chem. Mater. 21 (2009) 1253–1259.
[22] K. Zhou, et al., Synthesis, characterization and catalytic properties of CuO nanocrystals with various shapes, Nanotechnology 17 (2006) 3939–3943.
[23] M.L. Zhong, et al., Synthesis, growth mechanism and gas-sensing properties of large-scale CuO nanowires, Acta Mater. 58 (18) (2010) 5926–5932.
[24] Y. Liu, et al., From copper nanocrystalline to CuO nanoneedle array: synthesis, growth mechanism, and properties, J. Phys. Chem. C 111 (13) (2007) 5050–5056.
[25] Q. Zhang, et al., Facile large-scale synthesis of vertically aligned CuO nanowires on nickel foam: growth mechanism and remarkable electrochemical performance, J. Mater. Chem. 2 (11) (2014) 3865.
[26] Y. Wang, et al., Formation of CuO nanowires by thermal annealing copper film deposited on Ti/Si substrate, Appl. Surf. Sci. 258 (1) (2011) 201–206.
[27] K. Zhang, et al., Synthesis of large-area and aligned copper oxide nanowires from copper thin film on silicon substrate, Nanotechnology 18 (27) (2007) 275607.
[28] M.R. Morales, L.E. Cadus, Cooper foils used as support for catalytic monoliths. Superficial nano/microstructures obtained for two treatments, Catal. Today 213 (2013) 171–182.
[29] J. Liang, et al., Thin cuprous oxide films prepared by thermal oxidation of copper foils with water vapor, Thin Solid Films 520 (7) (2012) 2679–2682.
[30] J. Liang, et al., The synthesis of highly aligned cupric oxide nanowires by heating copper foil, J. Nanomater. 2011 (2011) 1–8.
[31] J. Gao, et al., Influence of crystal orientation on copper oxidation failure, Appl. Surf. Sci. 255 (11) (2009) 5943–5947.
[32] S.K. Shinde, et al., Hierarchical 3D-flower-like CuO nanostructure on copper foil for supercapacitors, RSC Adv. 5 (2015) 4443–4447.
[33] Y. Yang, et al., *Cu_2O/CuO bilayered composite as a high-efficiency photocatode for photoelectrochemical hydrogen evolution reaction*, Sci. Rep. 6 (2016) 35158.
[34] K. Pijus, et al., Wet chemically synthesized CuO bipods and their optical properties, Recent Patents on Nanotechnology 10 (1) (2016) 20–25.
[35] A. Bhaumik, et al., Significant enhancement of optical absorption through nanostructuring of copper based oxide semiconductors: possible future materials for solar energy applications, Phys. Chem. Chem. Phys. 16 (2014) 11054–11066.
[36] W. Zheng, et al., The phase evolution and physical properties of binary copper oxide thin films prepared by reactive magnetron sputtering, Materials 11 (2018) 1253.
[37] Y. Nakano, et al., *Optical bandgap widening of p-type Cu_2O films by nitrogen doping*, Appl. Phys. Lett. 94 (2009) 022111.
[38] Y. Wang, et al., *Transmittance enhancement and optical band gap widening of Cu_2O thin films after air annealing*, J. Appl. Phys. 115 (2014) 073505.
[39] D.S. Murali, et al., *Synthesis of Cu_2O from CuO thin films: Optical and electrical properties*, AIP Adv. 5 (2015) 047143.
[40] L.A. Alfonso-Herrera, et al., *Hybrid $SrZrO_3$-MOF heterostructure: surface assembly and photocatalytic performance for hydrogen evolution and degradation of indigo carmine dye*, J. Mater. Sci. Mater. Electron. 29 (12) (2018) 10395–10410.

[41] A.M. Huerta-Flores, et al., *Green synthesis of earth-abundant metal sulfides (FeS_2, CuS, and NiS_2) and their use as visible-light active photocatalysts for H_2 generation and dye removal*, J. Mater. Sci. Mater. Electron. 29 (13) (2008) 11613–11626.

[42] A. Soto-Arreola, et al., *Comparative study of the photocatalytic activity for hydrogen evolution of MFe_2O_4 (M= Cu, Ni) prepared by three different methods*, J. Photochem. Photobiol. A Chem. 357 (2018) 20–29.

[43] A. Soto-Arreola, et al., *Improved photocatalytic activity for water splitting over MFe_2O_4-ZnO (M = Cu and Ni) type-II heterostructures*, J. Photochem. Photobiol. A Chem. 364 (2018) 433–442.

[44] A.M. Huerta-Flores, et al., *Visible-light-driven $BaBiO_3$ perovskite photocatalysts: Effect of Physicochemical properties on the photoactivity towards water splitting and the removal of rhodamine B from aqueous systems*, J. Photochem. Photobiol. A Chem. 368 (2019) 70–77.

[45] O.A. Carrasco-Jaim, et al., Synthesis and characterization of PbS/ZnO thin film for photocatalytic hydrogen production, J. Photochem. Photobiol. A Chem. 347 (2017) 98–104.

[46] J. Juodkazyte, et al., *Study on copper oxide stability in photoelectrochemical cell composed of nanostructured TiO_2 and CuO_x electrodes*, Electrochim. Acta 137 (10) (2014) 363–371.

[47] M. Sun, et al., *A nanocomposite of carbon quantum dots and TiO_2 nanotube arrays: enhancing photoelectrochemical and photocatalytic properties*, RSC Adv. 4 (2014) 1120–1127.

[48] M.A. Mahadik, et al., *Fabrication of a ternary $CdS/ZnIn_2S_4/TiO_2$ heterojunction for enhancing photoelectrochemical performance: effect of cascading electron-hole transfer*, J. Mater. Chem. 3 (2015) 23597–23606.

[49] S.Y. Chae, et al., *Improved photoelectrochemical water oxidation kinetics using a TiO_2 nanorod array photoanode decorated with graphene oxide in a neutral pH solution*, Phys. Chem. Chem. Phys. 17 (2015) 7714–7719.

[50] Z. Zhang, et al., Highly stable copper oxide composite as an effective photocathode for water splitting via a facile electrochemical synthesis strategy, J. Mater. Chem. 22 (2012) 2456.